PROCEEDINGS OF SPIE

Status and performance of Lowell Observatory's Lowell Discovery Telescope's active optical support system

Cornelius, Frank, Sweaton, Michael, Hardesty, Ben, Collins, Michael, Levine, Stephen

Status and performance of Lowell Observatory's Lowell Discovery Telescope's active optical support system

Frank Cornelius[a], Michael Sweaton[a], Ben Hardesty[a,b], Michael Collins[a], and Stephen E. Levine[a,c]

[a]Lowell Observatory, 1400 West Mars Hill Road, Flagstaff, AZ 86001, USA
[b]Montana Instruments Corp., 101 Evergreen Drive, Bozeman, MT 59715, USA
[c]Dept. of Earth, Atmospheric, and Planetary Sciences, Massachusetts Institute of Technology, 77 Massachusetts Ave. Cambridge, MA 02139, USA

ABSTRACT

Lowell Observatory's Lowell Discovery Telescope (LDT) is a 4.3-m telescope designed and constructed for optical and near infrared astronomical observation. We examine the performance of the primary and secondary mirror support systems during scientific operations, over the first six years of science operations. During that time we have redesigned the sacrificial pins in the primary mirror lateral support system, and developed a method to re-calibrate the load cell sensors used in both the primary and secondary mirror supports.

Keywords: LDT, Lowelll Discovery Telescope, Lowell Observatory, Telescope and systems performance, System status, Optical support systems, Load cell calibration

1. INTRODUCTION

Lowell Observatory's Lowell Discovery Telescope (LDT; formerly named the Lowell Discovery Channel Telescope – DCT) is a 4.3-m telescope designed and constructed for optical and near infrared astronomical observation. The LDT has been in full science operation since the beginning of 2015, and mixed science and commisioning for three years prior to that. With an instrument assembly at the f/6.1 Cassegrain focus the LDT is capable of carrying up to five instruments. See Ref. 1 for an overview of the basic site and facility parameters, and Refs. 1–4 for discussions of various aspects of the facility and its performance. Since the last report, LDT has seen the addition of two new instruments, the Quad-camera Wavefront-sensing Stellar Speckle Interferometer (QWSSI)[5] and the Lowell Observatory Solar Telescope (LOST),[6] which feeds the EXPRES spectrograph.[7]

In this contribution we examine the performance of the primary and secondary mirror support systems during scientific operations, over the first eight years of operations.

The LDT primary mirror is a 4.3-m diameter thin meniscus mirror cast by Corning and figured by the University of Arizona Optical Sciences Center.[1] The Active Optics System[8,9] is responsible for the maintaining the position and figure of the primary and secondary mirrors. The primary mirror vertical position and figure are controlled by 120 axial actuators; the drive train consist of a stepper motor, harmonic drive, and ballscrew. Force feedback is provided by a load cell sensor mounted at the top of the actuator. Lateral positioning is controlled by a set of 36 pneumatic actuators mounted in a Schwesinger style configuration.[10] Force feedback is provided by three tangent definers; these define the mirror x, y position and rotation.

Two issues with the mirror supports have emerged since LDT started regularly operating. The first, described in section 2, is the failure of sacrificial pins designed into the primary mirror lateral support positioning feedback system. We have had more pin failures than expected which led to an analysis of the causes of failure and a redesign of the pin.

The second issue with the mirror support systems has been drift of the electrical zero point of the load cell sensors which we discuss in section 3. The load cells are integral to control of the telescope optics. They provide force feedback to the primary mirror axial supports which maintain primary mirror position and shape. They also provide position feedback for the the secondary mirror supports.

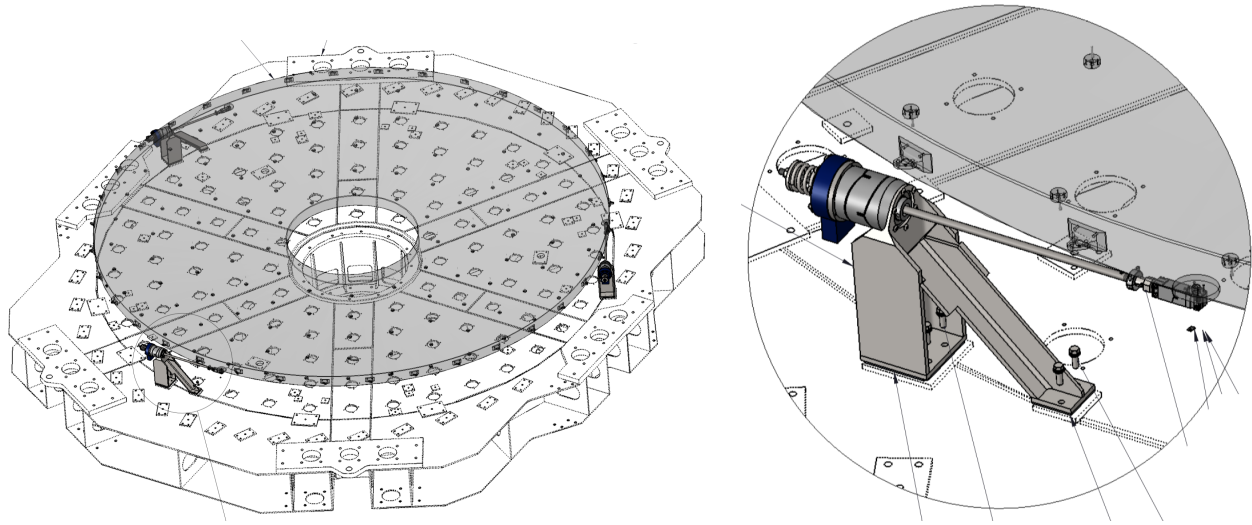Corresponding author S.E.L.: Email: sel@lowell.edu

Figure 1. *Left*: Schematic showing the primary mirror and locations of the tangent definer assemblies. *Right*: Expanded view of a tangent definer assembly. The right end of the arm clamps onto the tangent definer pin, which mates with the puck that is bonded to the back side of the mirror.[11]

2. SACRIFICIAL TANGENT PINS

Three tangent definers provide the feedback to the primary mirror lateral positioning system. The sacrificial pins that are used to connect the primary mirror to the tangent defining rods were designed as a fail safe, to prevent the application of overly large lateral stresses on the primary mirror.
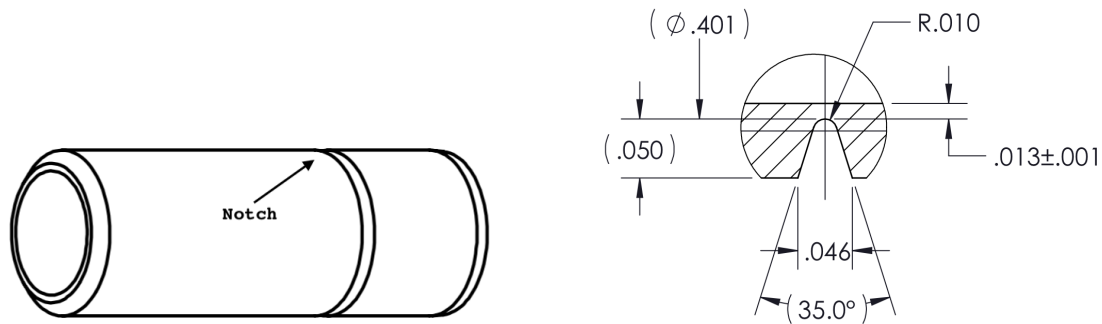

Figure 2. *Left*: Schematic showing the original pin design. *Right*: Expanded view of the notch that was designed in as the breaking point of the pin.[12]

In the original design (see Fig. 2), the pins were designed to press fit into the central hole in the tangent definer pucks, which are bonded to the back of the mirror. The portion of the pin extending beyond the puck is clamped by the end of the tangent definer rod. The original pins were made from Invar 36, and had to be fabricated to very tight tolerances. A number of pins were tested to failure on the bench after fabrication. One consequence of the tight tolerances was a wider than desired range of actual breaking forces.

Over the past 8 years of operations, the sacrificial pins have broken more frequently than we expected. The process of replacing the pins brought to light a potential difficulty with the original design if we needed to replace pins more frequently than the original design lifetime. The pins and pucks are both made from annealed Invar

36 which is difficult to machine, and there are only a limited number of manufacturers able to work with the material. The pin was press fit into the center hole in the puck. The process of removing a broken or damaged pin ran the risk of galling the inside surface of the hole, which would require replacing the puck (which is epoxied to the mirror and would entail significantly greater effort and downtime).

Further analysis of the force logs from the mirror support system indicated that typically the pins failed at the end of a night during shutdown; the recorded forces were higher than expected but within nominal tolerances. It appears that the pins were subject to cycle fatigue. In the past, we have been able to replace pins within a period of several hours, thus salvaging the latter portions of the nights impacted by pin breakages.

For the reasons noted above of cost, tight fabrication tolerances to meet the tight window in breaking force, and worries about the possibility of damaging the pucks (which are bonded to the glass) during pin replacement, we decided to redesign the pins.

In the process of the redesign, we added a cycle fatigue test to the validation of the new design. As part of that, we constructed a bench test allowing us to test for the cycle fatigue that we believe caused the premature failures in the original pins.

2.1 Design Criteria

The aim was to come up with a new design that was more resistant to cycle fatigue, and that simplified the manufacturing of the pins and the replacement procedures. In addition to the shear force breaking criterion, we added a requirement for longevity against low cycle fatigue. The computed safe maximum shear force for breaking the pins was set at 1,500 lbs, which is $\sim 80\%$ of the force that would generate the acceptable safe stress on the glass transmitted through the definer puck.
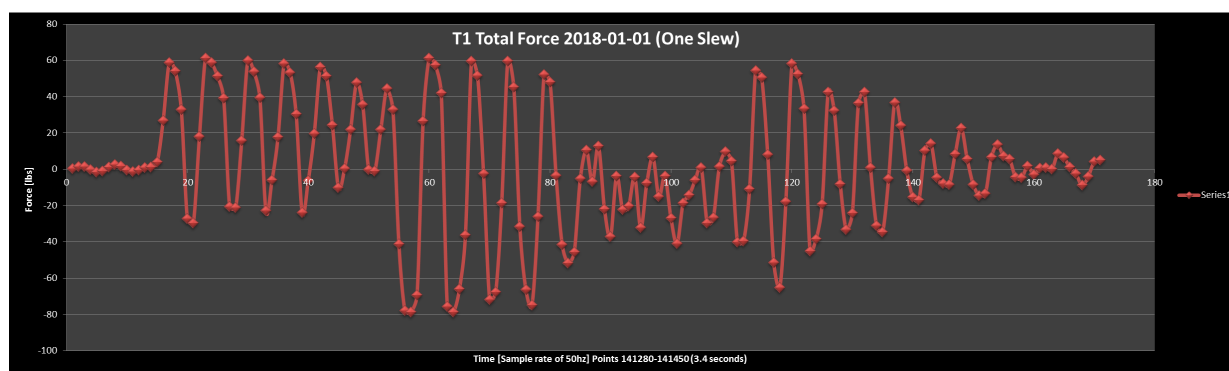

Figure 3. Typical variation of the forces recorded by the tangent definer load cells over the course of stopping a slew of the telescope. The plot covers 3.4 seconds of time. The maximum forces are within the system limits of ± 100 lbs.[13]

The cycle fatigue requirements were derived from the forces seen during the starting and stopping of a slew of the telescope, and the ringing that follows as the telescope velocity changes from slew to tracking speed (or vice versa, or a full stop; see Fig 3). Typical time for the ringing to damp is on the order of 3 to 4 seconds during which the tangent definers will see loads as high as ± 80 lbs, over roughly 20 full cycles. Velocity and acceleration changes are smoothed with an S-curve, which helps mitigate, but does not eliminate the ringing since the mirror mount is not perfectly rigid. Under the assumptions that LDT performs 40 slews per night, and is operational 340 nights each pin should see approximately full 272,000 cycles per year; this assumes ringing at start and stop, and that only half the cycles are full amplitude. For the desired mean time between failure (MTBF) of 2 years, that means that a pin should withstand roughly 544,00 cycles. When testing the MTBF for a sample of the new pins, we increased the number of test cycles by 20% for a minimum test run of 660,000 cycles.

2.2 Material Selection and Installation and Removal

Because of the previously noted difficulties working with Invar and the potential of damaging the puck that is bonded to the mirror, we considered both other materials and an alternate design for attaching the pin to the puck. A critical aspect contributing to the tight fabrication tolerances with the original pin design was the small cross-sectional area of the designed weak point. Small variances in the manufacturing could lead to large variations in the breaking strength. We looked for an alternate material where the cross-sectional area would be significantly larger for the same breaking strength, thus reducing the sensitivity to slight variations in the manufacturing. We ended up choosing to work with Aluminum 6061 T6. The cross-sectional area to shear at a standard break away force was $0.0345\,\mathrm{in}^2$, which 72% larger than the $0.0200\,\mathrm{in}^2$ area for annealed Invar 36.
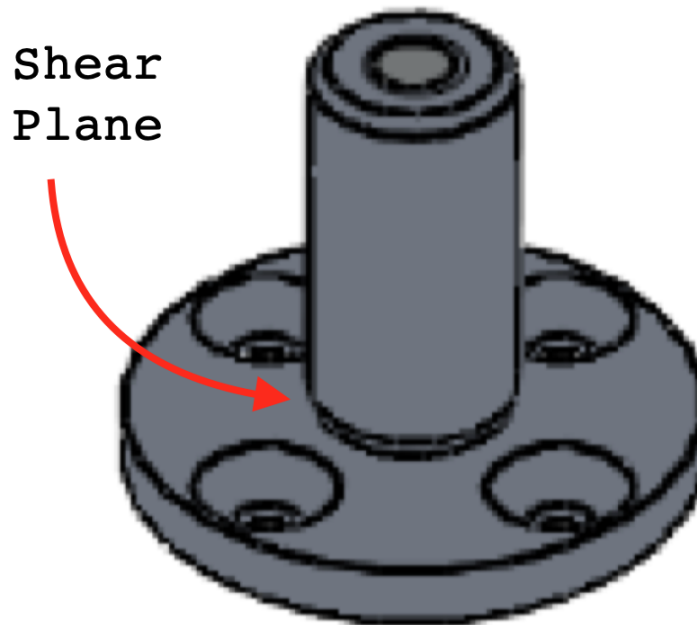

Figure 4. Schematic showing the new pin design.[13] The shear plane is defined by a machined groove where the cylinder meets the mounting plate.

Because the tangent definer pucks already have four accessible #8-32 threaded holes, we were able to modify the attachment method. Instead of a push fit pin, we added a flanged base to the pin with counter-sunk holes that matched the existing pattern (see Fig 4). The pin now is attached to the puck using $4 \times$ #8-32 fasteners, making installation and removal a much simpler and safer operation. The shear plane is machined in the base of the cylindrical portion of the pin.

2.3 Shear and Fatigue Testing

To determine the optimal cross-section, we constructed several versions of the sacrificial pin with differing cross-sectional areas (CSA). These were then tested to breaking. From the fit of CSA versus observed breaking force (Fig 5), we settled on a design with a CSA of $0.0530\,\mathrm{in}^2$, which should break at 1,500 lbs.

Three pins with the optimal CSA were then fabricated and subjected to cycle fatigue testing. We built a test jig (Fig 6) that allowed us to apply an adjustable cyclic force to the test pins. We tested the pins to a minimum of 660,000 cycles at $\pm 85\,\mathrm{lbs}$. The initial setup for the first pin was incorrect, so that pin was re-fatigued to the proper specs. None of the three pins failed during fatigue testing (Table 1). While we cannot deduce a MTBF from this, we can say that it should be greater than 2 years.

After putting the test pins through the fatigue test, they were then subjected to a shear test to confirm the breakaway force required to cause them to shear. In all three cases, the pins sheared within $\pm 50\,\mathrm{lbs}$ of the target
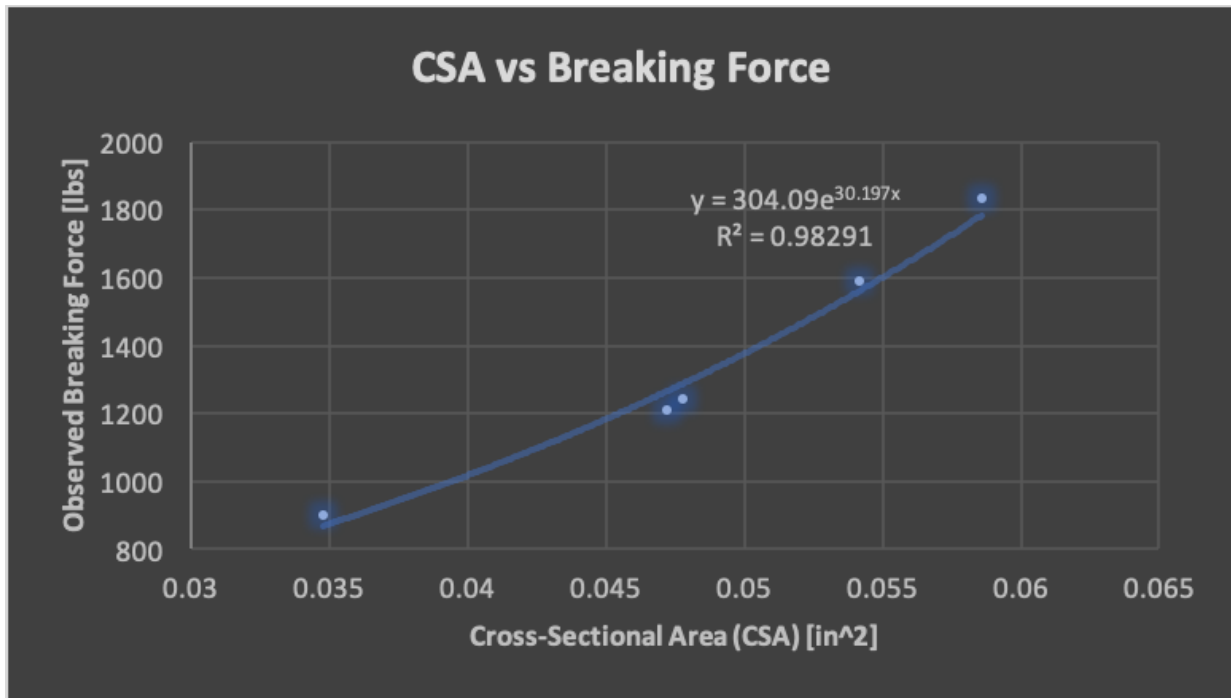
Figure 5. Plot of cross-sectional area [in^2]versus observed breaking force [lbs].[13]

Figure 6. The jig set up for fatigue testing of the pins. The pin is on the right. The pin end is visible within the clamp, and part of the pin flange can be seen above the body of the clamp.[13]

Table 1. Fatigue and shear test details.

Pin #	Cycles	Force [lbs]	Fatigue Results	Shear Force [lbs]
1	660,000	−60 to +85	No breakage	$\cdots$
1	660,000	−85 to +85	No breakage	1451.94
2	660,000	−85 to +85	No breakage	1486.51
3	660,000	−85 to +85	No breakage	1521.08

1,500 lbs (see Table 1). The pin (#1) with the lowest (and most discrepant) breaking force was the pin that was subjected to the extra round of cycling, and even after that still was within 50 lbs of the target shear force.

The new pins meet the overriding requirement of mirror safety. We are satisfied that the new design also meets our updated requirements for manufacturing, shearing consistency, ease and safety of replacement and MTBF.

3. LOAD CELL RECALIBRATION

The LDT active optics system (AOS) uses load cells in all its main subsystems to provide force feedback in the closed loop control of the actuators. Per the manufacturer, the load cells in use are supposed to be re-calibrated on the bench annually. For the units in use, this is not feasible, as we would need to remove the mirrors to physically access the load cells. The impact of drift in the load cell electrical zero point calibrations is still being assessed. At the very least, we expect that the drift in calibration will add a random noise component to the position definition. Since the load cells are all the same design, we assume there is likely to be a systematic contribution to the noise budget as well. All of this is expected to degrade the ability of the AOS to maintain proper alignment of the optics and figure of the primary mirror.
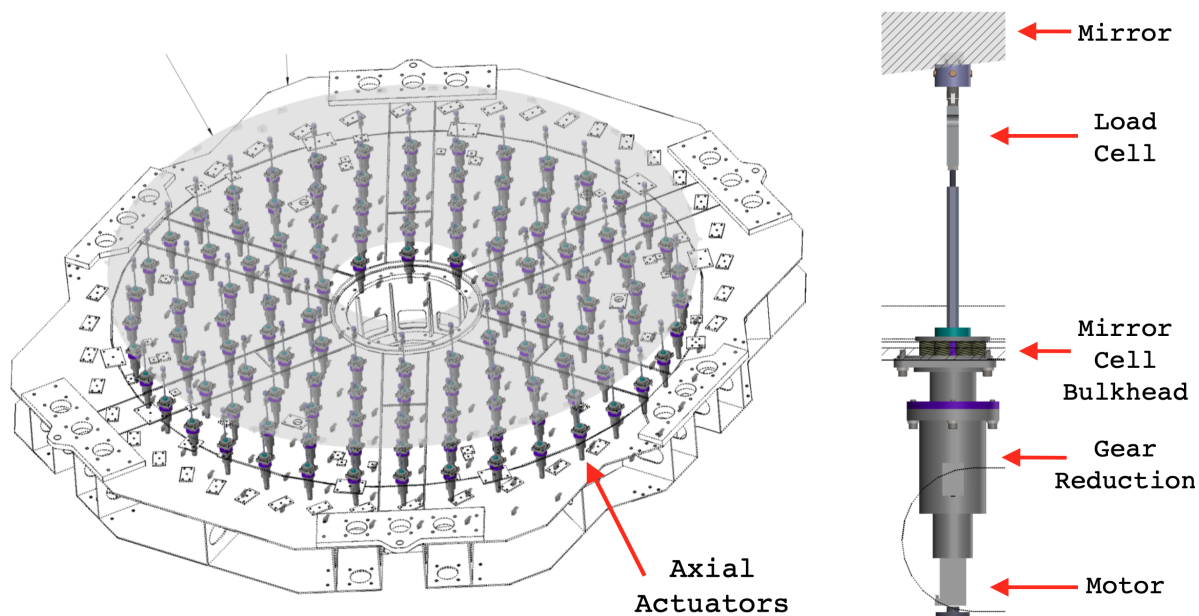

Figure 7. *Left*: Schematic showing the primary mirror and locations of the 120 axial supports. *Right*: Expanded view of a single axial actuator assembly. The load cell is mounted just below the tip of the actuator where is attaches to the back of the primary mirror.[11]

To address the issue, we have developed a method to re-calibrate the load cell sensors used in the primary mirror supports while they are in place. We have implemented this recalibration in July 2019 and August 2020 and plan to repeat this process annually. The load cells will also be fully re-calibrated in place every time we remove the primary and secondary mirrors for realuminization. To do this we will be constructing a test fixture that can be installed on top of each load cell permitting direct calibration of both offset and span.

The primary mirror (M1) support structure is made up of 120 axial and 36 lateral actuators (see Fig 7, left). The axials have integral load cell sensors near the tip where they attach to the backside of the primary mirror (see Fig 7, right). The electrical chain for each axial actuator feedback system consists of a load cell, a signal conditioning module, variable length wiring and an A/D converter. The load cells can operate in both

compression and tension. The output signal range has been calibrated so that ±10 Vdc corresponds to force loads in the range ±100 lbs.

As noted above, to fully re-calibrate the axial support load cells for would require removing the primary mirror so we can physically place the test jig on each. That in turn would require removing the entire mirror cell. Instead, the software that controls the axial supports includes a modifiable table of offsets for each axial support which can be used to correct for accumulated errors in the electrical stack up of the feedback subsystem. To adjust this, we developed a process to determine the updated electrical offset.

The recalibration process is iterative and depends upon knowing the total mass of the mirror and what the unmodified distribution of the mirror mass should be. Procedurally, we start with the telescope pointed at the zenith. For the LDT, the base configuration should distribute the load of M1 uniformly across the axial supports. The table of offsets is updated for the telescope pointing at an elevation of 90°. The lateral supports are also energized to keep M1 in its proper x, y position.

The M1 axial supports are arranged in 5 concentric rings and the load on each actuator is roughly equal, and we know the total mirror mass. The possible impact of curvature of the mirror on the distribution of the loads was checked and confirmed to be negligible. Because the load is expected to be distributed uniformly, we have a baseline that we can compare the measured loads against.

	(lbf) Ex Ret	(lbf) Ex Ret	(lbf) Ex Ret		(lbf) Ex Ret	(lbf) Ex Ret	(lbf) Ex Ret
A	57.7	57.7	57.6	A	57.8	57.8	57.8
B	57.7	57.7	57.7	B	57.8	57.8	57.8
C	57.7	57.7	57.6	C	57.8	57.8	57.8
D	57.7	57.7	57.7	D	57.8	57.8	57.8
E	57.7	57.7	57.7	E	57.8	57.8	57.8
F	57.7	57.6	57.7	F	57.8	57.8	57.8
G	57.7	57.6	57.6	G	57.8	57.8	57.7
H	57.7	57.6	57.6	H	57.8	57.8	57.8
J	57.7	57.7	57.7	J	57.8	57.8	57.8
K	57.7	57.7	57.7	K	57.8	57.8	57.8
L	57.6	57.7	57.7	L	57.8	57.8	57.8
M	57.7	57.6	57.6	M	57.8	57.8	57.8
N	57.6	57.7	57.7	N	57.8	57.8	57.7
P	57.7	57.7	57.7	P	57.8	57.8	57.8
Q	57.7	57.7	57.7	Q	57.8	57.8	57.8
R	57.7	57.7	57.6	R	57.8	57.8	57.8
S	57.7	57.7	57.7	S	57.8	57.8	57.8
T	57.7	57.7	57.6	T	57.8	57.8	57.7
U	57.7	57.7	57.6	U	57.8	57.8	57.8
V	57.6	57.7	57.7	V	57.8	57.8	57.8

Figure 8. Sample force data for half of the M1 axial supports measured before recalibration in July 2019 (*Left*), and after recalibration (*Right*). The expected value should be 57.8 lbs.

The difference between the measured and the theoretical forces is assumed to be caused by the drift in the overall combined errors for each actuator's feedback chain. The measured value already includes the current offset value. For our system, since the conversion factor is 1 Vdc/10 lbs, the offset voltage is found by dividing the residual force by 10.

If all loads are within 0.1 lbs of the expected value, we are done. If not, then for each actuator where the discrepancy exceeds this, we record the offset, zero out the offset for each discrepant actuator in the offsets table and restart the AOS. The difference between the measured and theoretical forces rescaled by the gain becomes the new offset for each discrepant actuator. Those values are entered into the offset table, and the measurements are repeated. For any actuators still discrepant, we repeat the process. In theory, we could repeat this until it converges, but in practice a second iteration is rarely needed. The reason that multiple iterations might be needed is because the actuators are linked by the glass, and so changes in the zero point for one will affect its neighbors in the second order.

The LDT primary mirror mass is 6,936 lbs. Dividing the total mass over 120 actuators gives 57.8 lbs per actuator. Before recalibration in July of 2019, most of the force zero points had drifted down by 0.1 to 0.2 lbs (Fig 8, left). After recalibration, the zero points were all nominal (Fig 8, right).

This process allows us to regularly correct for drift of the electrical zero points over time. The load cells also have a span that can drift over time. For the span, we will validate (and if needed recalibrate) each actuator using the test fixture on each load cell the next time that we remove the primary mirror for re-coating. As the typical relative forces tend to be moderate, the drift in zero point is expected to be a first order effect, while drift in span should be second order.

The combination of the re-designed pins and the in-situ load cell recalibration procedures has made the LDT primary mirror support system more robust, accurate and easier to maintain.

ACKNOWLEDGMENTS

REFERENCES

[1] Levine, S. E., Bida, T. A., Chylek, T., et al., Status and performance of the Discovery Channel Telescope during commissioning, Proc. SPIE, 8444, 844419 15pp. (2012)

[2] DeGroff, W. T., Levine, S. E., Bida, T. A., et al., Status and performance of the Discovery Channel Telescope from commissioning into early science operations, Proc. SPIE, 9145, 91452C 18pp. (2014)

[3] Levine, S. E, DeGroff, W. T., Status and imaging performance of Lowell Observatory's Discovery Channel Telescope in its first year of full science operations, Proc. SPIE, 9906, 9906-72 16pp. (2016)

[4] Levine S. E., DeGroff W. T., Bida T. A., Dunham E. W., Jacoby G. H., Status and performance of Lowell Observatory's Discovery Channel telescope and its growing suite of instruments Proc. SPIE, 10700, 107004P 12pp. (2018)

[5] Clark, C. A., van Belle, G. T., Horch, E. P., Trilling, D., Z. Hartman, The optomechanical design of the Quad-camera Wavefront-sensing Stellar Speckle Interferometer (QWSSI), Proc. SPIE, 11446, 11446-55 (this meeting) (2020)

[6] Llama, J., The Lowell Observatory Solar Telescope to observe the Sun as an exoplanet host star with the EXtreme PREcision Spectrograph, Proc. SPIE, 11445, 11445-272 (this meeting) (2020)

[7] Jurgenson, C. A., Fischer, D. A., McCracken, T. M., et al., EXPRES: a next generation RV spectrograph in the search for earth-like worlds, Proc. SPIE, 9908, 99086T 20pp. (2016)

[8] Smith, B., Chylek, T., Cuerden, B., Degroff, B., Lotz, P. J., Venetiou, A., The active optics system for the Discovery Channel Telescope, Proc. SPIE, 7739, 77391T 21pp. (2010)

[9] Venetiou, A. J., Bida, T. A., Discovery Channel Telescope Active Optics System Early Integration and Test, Proc. SPIE, 8444, 84441E 11pp. (2012)

[10] Schwesinger, G., Lateral support of very large telescope mirrors by edge forces only, JMOp, 38, 1507 (1991)

[11] French, J., DCT M1 Support Structure, Tangential Definer Assembly (drawing), DCT-0301D-062-5 (2011)

[12] Chylek, T., DCT M1 Assembly – Sacrificial Pin (drawing), DCT-0380D-005-2 (2012)

[13] Cornelius, F., DCT M1 Flanged Base Tangent Definer Sacrificial Pin, DCT-0301D-XXX (2019)